Fachtagung "Lasermethoden in der Strömungsmesstechnik"
8. – 10. September 2015, Dresden

Visualisierung der 2-Phasen-Strömung in einer PEM-Elektrolyse-Zelle durch Neutronenradiographie

Visualization of the two-phase flow inside a polymer electrolyte membrane water electrolysis cell using neutron radiography

Alexander Spies[1,6*], Michael A. Hoeh[2], Tobias Arlt[3] , Nikolay Kardjilov[3], David L. Fritz[2], Jannik Ehlert[2], John Banhart[3,4], Manuel Münsch[6], Antonio Delgado[6], Alexander Hahn[1], Ingo Manke[3], Werner Lehnert[2,5]

[1] Siemens AG, Hydrogen Solutions, 91052 Erlangen
[2] Forschungszentrum Jülich GmbH, Institute of Energy and Climate Research, IEK-3: Electrochemical Process Engineering, 52425 Jülich, Germany
[3] Helmholtz-Zentrum Berlin GmbH, Institute of Applied Materials, Hahn-Meitner-Platz 1, 14109 Berlin, Germany
[4] Technische Universität Berlin, Hardenberg Str. 36, 10623 Berlin, Germany
[5] Modeling in Electrochemical Process Engineering, RWTH Aachen University, 52056 Aachen, Germany
[6] Institute of Fluid Mechanics, Friedrich-Alexander University Erlangen-Nuremberg, 91058 Erlangen
*corresponding author, alexander.spies@siemens.com

Elektrolyse, PEM, Gasdiffusionsschicht, 2-Phasen-Strömung, Neutronen-Radiographie
Electrolysis, PEM, gas diffusion layer, two-phase flow, neutron radiography

Abstract

With the increasing percentage of renewable energy sources in the overall electricity production – especially in Germany – the load leveling of electric energy due to the volatile character of renewable energy sources compared to conventional energy sources like coal or natural gas becomes more and more important. One option of storing electrical energy over the short term, and also over days and weeks, is to convert the energy to hydrogen using electrolysis. Especially PEM[1]-electrolysis offers a high degree of flexibility and at the same time a high purity of the produced hydrogen. One of the core components of a PEM-electrolysis cell is the gas diffusion layer (GDL, also referred to as the current collector or porous transport layer in literature). This enables the distribution of the electric current and at the same time supports the removal of the evolving gases. Due to the high current densities during cell operation, massive metal structures are necessary, and it is not possible to visually observe the two-phase flow processes inside of the cell without disturbing the flow field or the distribution of the electric current. One possibility to gain an insight into a running cell is to use neutron radiography. The two-phase flow at different operating conditions is examined in this paper and the results discussed. The influence of different cell conditions regarding the point of operation are also documented.

[1] PEM = Polymer Electrolyte Membrane

1. Introduction

Water electrolysis has been a field of growing interest in recent years due to its ability to store electricity generated from intermittent renewable sources like wind or solar energy. In this way it is possible to store larger amounts of energy compared to other technologies such as batteries or supercapacitors [9]. In PEM water electrolysis, water is supplied at the anode side and split into oxygen, electrons and protons. The protons are transported through the polymer electrolyte, while the evolving oxygen generated is transported out of the cell with the feed water as two-phase flow.
The operating pressure strongly influences the two-phase flow in terms of the evolving volumes. PEM water electrolysis is capable of producing hydrogen safely at a pressurized level of up to 100 bars [7]. A high operating pressure of the electrolysis leads to a small reduction of the electrolysis efficiency due to crossover effects over the membrane [8], but it allows reducing the costs for subsequent compression stages.
On the other hand, operation at lower pressure levels of the electrolysis cell itself decreases the cell costs, as it allows a much lighter design to be employed. The profitability of PEM electrolysis is a decisive factor for the future use cases of this process [6] and requires that the operating conditions are carefully evaluated. As a consequence, this work focuses on identifying the influence of different operating conditions, especially different internal pressures, on the cell performance. It also focuses on the two-phase flow processes inside the GDL at different operating conditions and at different positions on a single GDL.

2. Description of the visualization task

PEM water electrolysis systems are currently scaled to the Megawatt range, necessitating an increase of the active area of individual cells in order to reduce the overall costs [6]. This upscaling goes along with questions concerning how the media is distributed over large cell areas. Typically, a gas diffusion layer is used to allow a more homogeneous media distribution over the active cell area. The oxygen side of the current collector allows H_2O to be transported to the reactive zone and at the same time oxygen to be transported away from the electrode. Information about the oxygen saturation and distribution inside the current collector at different points of operation but also at different locations inside a homogeneous current collector are of special interest. Due to the continuous production of oxygen and hydrogen gas over the whole active area of the electrolysis cell – and therefore over the whole contacting area of the GDL – the gases move from the bottom to the top of the electrolysis cell where they accumulate (in the case of a vertical orientation). One option to visualize these effects would be to employ a transparent GDL material to allow optical inspection. However, this approach disturbs cell operation as the cell has to be electrically connected by establishing a connection on the side of the cell or otherwise by using electrical connectors through the cell. The former changes the current distribution and the latter disturbs the flow field. Therefore, a pure optical inspection falsifies the effects that are observed as a result of the perturbations that it introduces.

3. Non-invasive solution to the visualization task

There are methods that allow the cell structure and the processes inside a cell to be visualized at the same time using an unaltered cell setup, and employing standard metallic materials as is usually the case for the GDLs and for the surrounding parts such as the end plates. One of them is the non-invasive neutron radiography, where a neutron beam penetrates the cell, and the especially high neutron attenuation of hydrogen allows the

gas/water distribution to be visualized. This method has been successfully applied in the past to PEM fuel cells [1,3,4] and liquid-fed direct methanol fuel cells [2], where it allowed the water distribution inside operational cells to be studied. This technique has also recently been applied to PEM water electrolysis [5], where the water accumulation on the cathode side was studied. This technique allows the interior of large samples (up to hundreds of cubic centimeters) to be investigated with a spatial resolution of lower than 100 µm and a temporal resolution of up to 1 s. The ability of neutrons to be transmitted through several centimeters of metal on the one hand, and to be very sensitive to small amounts of light elements such as hydrogen, boron and lithium on the other hand, makes neutron radiography a unique method for non-destructive testing in both industry and materials science. Using this method, the gas/water distribution inside a PEM water electrolysis cell has been studied using neutron radiography at CONRAD (Helmholtz-Zentrum Berlin) for different operating conditions. Special focus has been placed on the dynamics in the transport and quantifying the distribution across the cell area and the oxygen content of the cell. To the knowledge of the authors this technique is employed for the first time to visualize flow processes during PEM water electrolysis on the anode side at different locations.

4. Experimental setup

All of the measurements are being carried out at the CONRAD-2 beamline at the BER II neutron source at Helmholtz-Zentrum Berlin under the following experimental conditions: detector system (sCMOS camera “Andor NEO”) with a pixel size of 22µm, scintillator screen (6LiFZnS) with a thickness of 100 µm and beam collimation ratio (L/D) of 350. The polymer electrolyte membrane water electrolysis cell is placed in the neutron beam and images were taken every second.

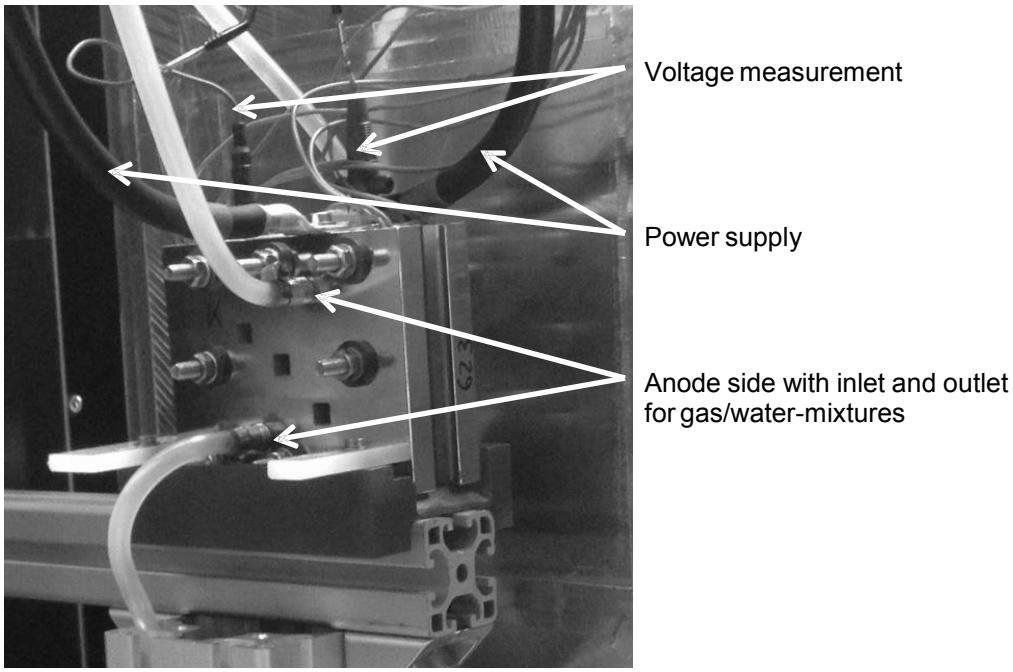

Figure 1: Experimental setup at CONRAD-2

Therefore, dynamic processes in the range of some seconds are visible; however, processes faster than 1 s cannot be resolved. Yet no further efforts have been made neither to increase the time resolution nor to correct possible data bias due to the relatively large exposition time. The setup consists of an electrolysis cell, which is a machined metal structure. Water and

oxygen gas – if needed to reproduce boundary condition over a large cell area – are pumped through the cell. Only the anode side is supplied with water and additional gas, the cathode side is not supplied with water. The cell installed in front of the detector is shown in Figure 1. On the cathode side, a graphite paper is installed as gas diffusion layer. The resulting measurements are a superposition of the anode and cathode side. The processes on the cathode side are not as dynamic as on the anode side as there is no circulating water and a much thinner gas diffusion layer (around 0.3 mm) when compared to the anode side (around 7 mm). Thus the dynamic effects on the anode side are much more significant, and can be studied independently of the cathode. The active area of the cells is 42 mm x 42 mm, which is equal to the size of the gas diffusion layer in the setup. The cell was operated at atmospheric pressure. The water flow rate was able to be adjusted. The flow is directed from the bottom to the top of the cell. To simulate pressurized conditions, where the evolving gas volumes are smaller, the measurements are done at lower current densities and atmospheric pressure to simulate the low gas percentage and the lower gas volumes when operating under pressure. The effect of the changes in gas density and kinematic viscosity on the dynamics of the two-phase flow has been neglected (see for example [10]). No measurements could be found for the effect of pressure on the surface tension at the oxygen/water interface. Similar measurements of the water/CO2 [12][14] and water/methane [13] combinations indicate for the given conditions that the influence was small; in the range of -10% for water/CO2, and about -7% for water/methane.

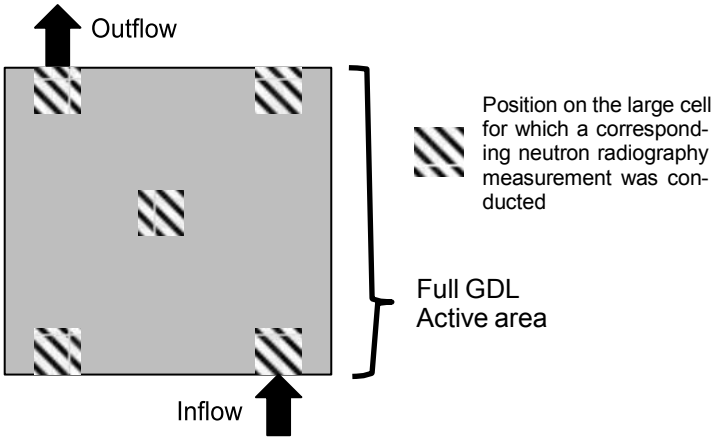

Figure 2: Positions on the large area cell corresponding to the neutron radiography measurements

The inlet and outlet flows are distributed over the width of the cell before they enter the cell. There is no separate flow field in the cell, as the gas diffusion layer provides the flow field functionality. The gas diffusion layer itself is composed of several layers of stretched metal mesh sheets. The electrical current is distributed from the end plate to the roughest layer with only a small number of contact points and to the finest layer with a much higher number of contact points over the sample.

The results of the measurements are images with different grayscale values, representing the intensities of the transmitted neutron beam at different locations on the image. The intensity predominantly depends on the amount of water that is irradiated, as the neutron attenuation in our setup is mainly due to water. An oxygen bubble evolving in water therefore leads to an increase in neutron transmission as the amount of water for the neutron beam to penetrate decreases, as does the neutron attenuation. Therefore, the oxygen bubbles lead to brighter spots in the image. A reference image (index R) was chosen where the cell is just perfused by water and current is not applied to the cell, i.e. without electrolysis being operational. This reference picture R is an averaged picture over 120 single pictures. In order to obtain a measure for the change in the amount of gas between two settings, all images (index M) were divided by the reference image R. For an isothermal process the beam attenuation over a thickness z of gas at one pixel (width Δx) of the picture follows the Beer-Lambert law

$$I_M(i,j) = I_0(i,j) \cdot \exp(-\alpha \cdot z)$$

where $I_0(i,j)$ is the initial beam intensity at the pixel location (i,j), $I_M(i,j)$ is the beam intensity after transmission through the cell and thus through the mixture of water and gas, α is the attenuation coefficient. In order to quantify the change in the water/gas ratio, this intensity $I_M(i,j)$ is divided by reference intensity $I_R(i,j)$. Therefore solving the resulting equation for the thickness z yields information about the gas volumes $V_{gas}(i,j) = \Delta x \cdot \Delta x \cdot z$ at the pixel location (i,j), so that

$$V_{gas}(i,j) = \frac{\Delta x^2}{\alpha} \cdot \ln\left(\frac{I_M(i,j)}{I_R(i,j)}\right)$$

The attenuation coefficient α comprises the attenuation coefficients of the water, of the gases, and the remaining cell components, so that $\alpha = \alpha_{H_2O} + \alpha_{O_2} + \alpha_{components}$. As the neutron attenuation primarily occurs in the hydrogen of water, only the contribution by water is considered, so $\alpha = \alpha_{H_2O}$. In the work carried out, a value of α = 5.2 cm^{-1} was determined by performing a calibration measurement for a defined distance of 5 cm between the measurement setup and the detector.

5. Results

Neutron radiography measurements have been conducted at different operating points of the cell being tested. These conditions reflect the conditions inside a complete electrolysis cell with an active area of 1400 cm2 (at 35 bar) and 15,000 cm² (atmospheric) respectively at different positions of this area (Figure 2) and at different current densities. Oxygen was additionally injected from the bottom of the measurement cell to reproduce the accumulation of oxygen from the bottom of the cell to the top. This setup therefore allows the gas/water distribution and transport to be studied, as it would actually occur in an electrolysis cell with a large active area.

5.1. Comparison between pressurized and atmospheric operation

In a first step, some of the points of operation are shown at their corresponding position inside a larger GDL. The focus is on the normal point of operation for an atmospheric and a simulated pressurized system (35 bar). Figure 3 shows the comparison at 5 different positions of a GDL in the size of 1.400 cm² (35 bar) and 15,000 cm² (atmospheric). When operating at atmospheric pressure, significant differences occur between inlet and outlet, which is obvious due to the accumulation of larger gas volumes compared to the simulated pressurized operation, where far lower gas volumes occur.

Two comparisons concerning the O_2 content in the open GDL volume (volume of the GDL available for water and gas) are shown in Fig. 4.

Operation under pressure – with focus on the O_2 content – is nearly independent of the O_2 input volume flow (left picture). This correlates with the observations during operation. Gas bubbles mostly grow until a specific size is reached, depending on the structure of the GDL. They are then driven out of the cell as a result of their inherent buoyancy. The duration of accumulation is 2-3 seconds depending on the current density. The gas content in the cell in pressurized operation fluctuates in a range of about ±10-15% (standard deviation) around the mean value.

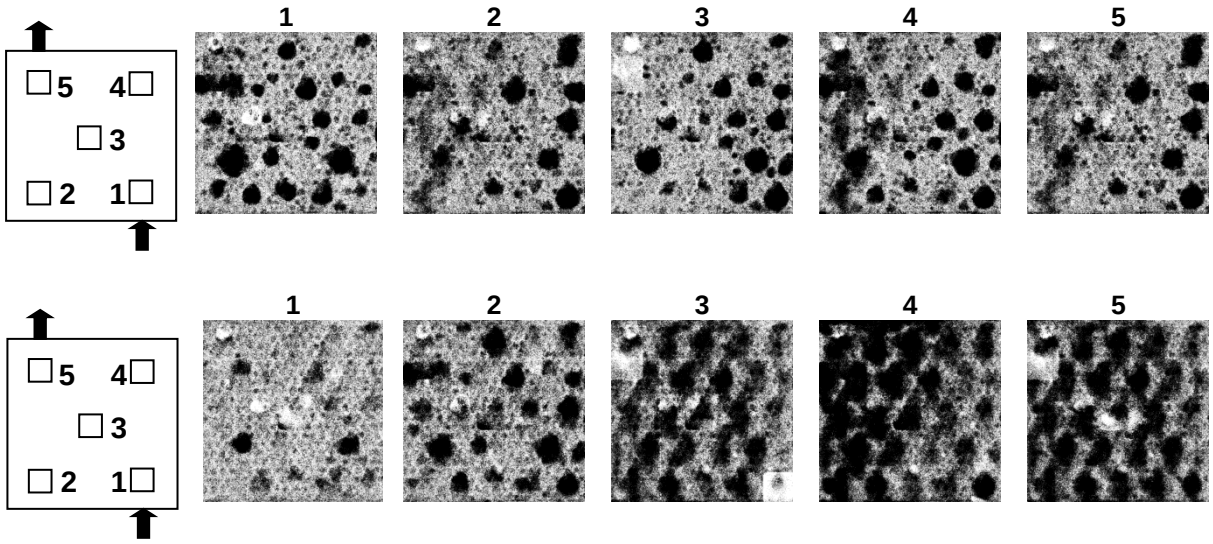

Figure 3: Comparison of the oxygen saturation when operating under pressure (35 bar, top) and at atmospheric pressure (bottom). Gas is shown in black for visualization purposes

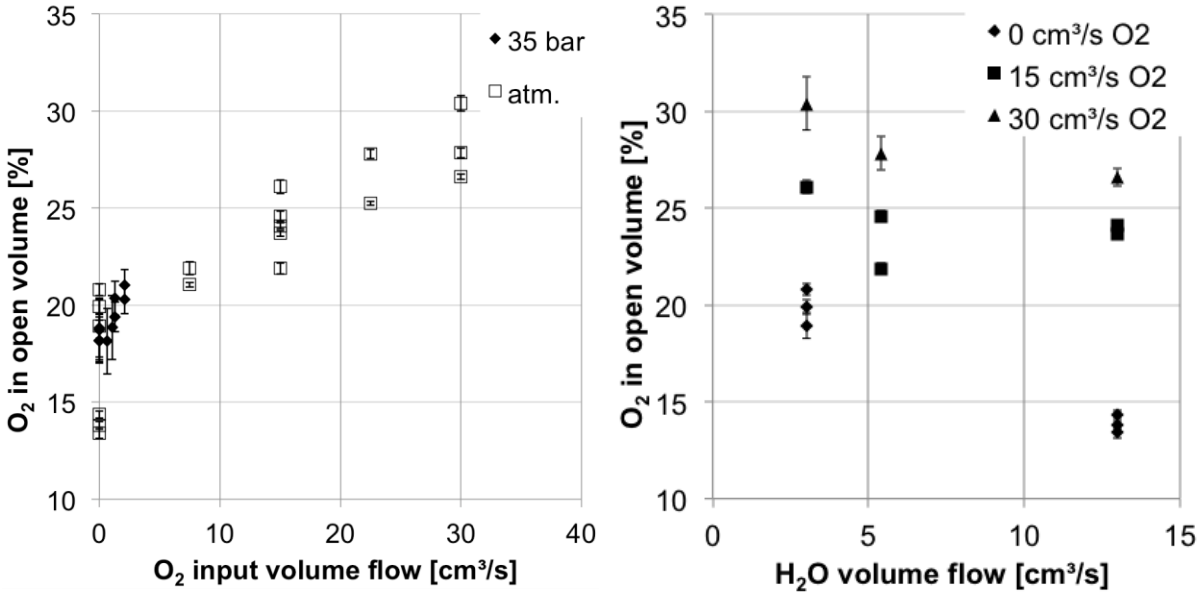

Figure 4: O_2 content in open GDL volume as a function of O_2 input flow (left) and H_2O input flow (right)

When operating at atmospheric pressure, the volumetric O_2 flow is much higher, which leads to a strong dependency between the O_2 input volumetric flow and the gas content inside the cell. The variations in the gas content are in the range of ± 1-3% (standard deviation) of the mean value, which is much smaller compared to the pressurized condition. The character of the flow turns from single arising bubbles (at pressurized condition) to a quasi-steady character (at atmospheric condition) of the oxygen content in the cell. This is due to the around 20-30 times higher volumetric gas flow rates, which lead in the end and for the whole cell to a smaller variation of the O_2 content in the electrolysis cell at atmospheric condition. This is independent of the observation of strongly different gas contents of the sample cells depending on the position in the larger GDL (see Figure 3).

The right-hand part of Figure 4 shows the relationship between the O_2 content in the open GDL volume and the H_2O input volume flow. As the H_2O flow increases, the O_2 content decreases.

5.2. Influence of gas percentage under steady operating conditions

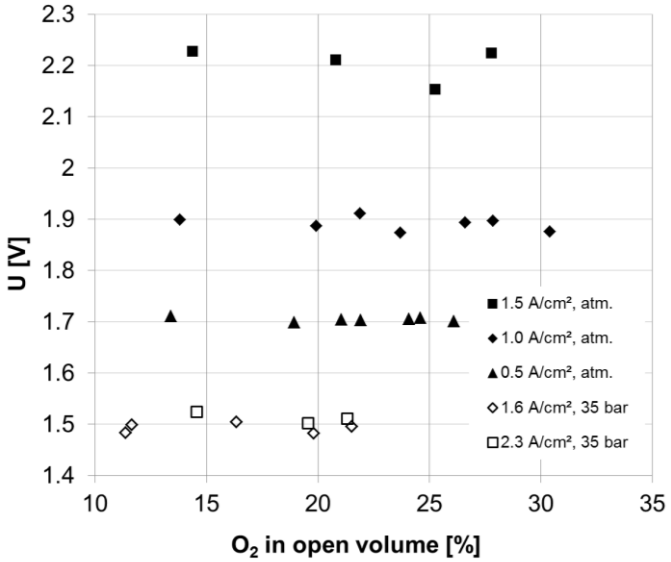

Figure 5: Cell voltage in dependence of the O2 content

The gas content in the cell with respect to the cell voltage for different operating points is shown in Figure 5, which also means different H_2O and O_2 input volume flows. A relationship to the cell performance comparable with the “dry-out” effect, which is common for fuel cells at high current densities (see for example [11]), was not observed. The cell performance seems to be independent of the gas content inside the cell, and therefore also from the location inside a bigger gas diffusion layer, at least for the selected conditions (which lead to a maximum O_2 content of about 30%).

5.3. Comparison of the dynamic behavior

The cell voltage after a change in current density is shown in Figure 7 when the cell is operating at atmospheric pressure. The current density was changed from 0.5 A/cm² to 1 A/cm² (dotted lines) and from 1 A/cm² to 1.5 A/cm² (solid lines). The operating state changes are different concerning water volume flow and oxygen volume flow. It can be seen that there are significant differences concerning the dynamic behavior. At the step from 0.5 to 1.0 A/cm², the operating point almost immediately reaches a steady state, while at the step from 1.0 to 1.5 A/cm², the operating point needs at least 20 min to reach a quasi- steady state. Up until now, the reason for this behavior is unclear and needs further investigation. One possibility is a lack of running-in time. Other measurement setups of the authors have shown a similar behavior during the running-in time. However, the situation did not change even after 10 hours in operation. A tendency to decrease during continuous operation of the cell was not able to be identified (see Figure 6, small diagram). The lack of performance could therefore also occur due to transport problems in the cell at higher current densities and when operating at atmospheric pressure.

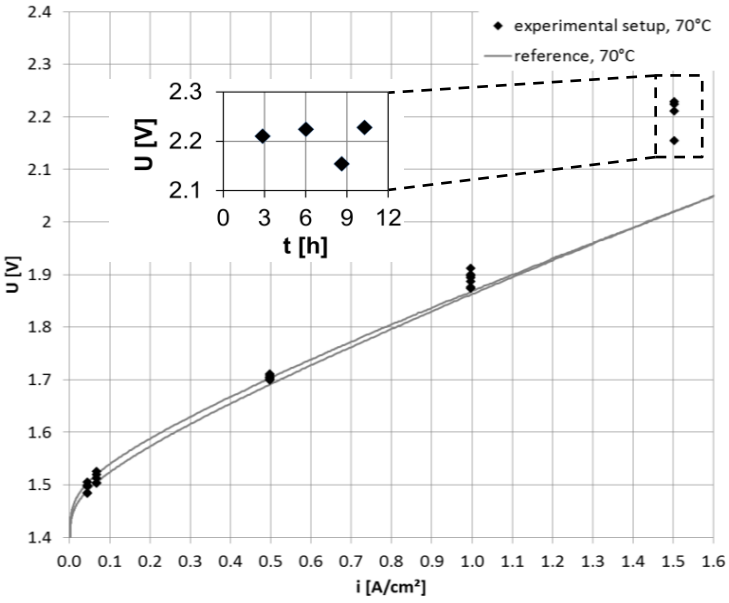

Figure 6: Current - voltage - characteristic of the setup

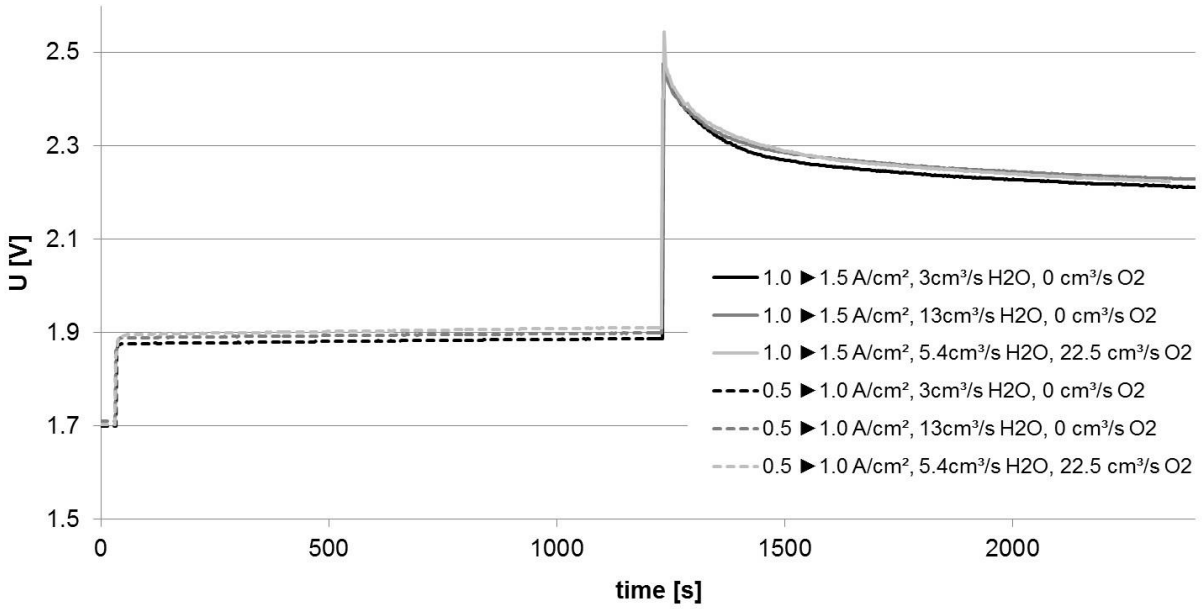

Figure 7: Voltage over time at different atmospheric conditions

6. Conclusions

The experiment at the Helmholtz-Zentrum Berlin presented in this paper shows one possibility of simulating different conditions within a larger GDL in order to get an overview over the two-phase flow inside a GDL. It has been found that the two-phase flows depend heavily on the location of the sample (inlet, outlet, center of the GDL) when operating at atmospheric pressure. No significant differences could be identified when operating under pressure. The volumes of oxygen were estimated by comparing the resulting flow pictures, which indicated average oxygen contents of about 18 to 21% when operating under pressure, and 14 to 30 % when operating at atmospheric pressure.
It has been concluded that the character of the flow field is nearly equal for different positions inside a GDL when operating under quasi-pressurized conditions (Figure 3, top pictures), and the fluctuations in oxygen saturation are in the range of ±10-15%. When operating at atmospheric pressure, the character of the flow field depends strongly on the position inside the GDL (Figure 3, bottom pictures); however, the oxygen saturation revealed to be more constant, with deviations of just ±1-3% of the mean value.
Another finding is that for steady-state operation (after about 20 min) the cell voltage is not dependent on the gas content in the open volume up to the gas content levels that could be reproduced. However, in dynamic operation there is a significant difference between jumps from 0.5 to 1.0 A/cm² and 1.0 to 1.5 A/cm² for the voltage when operating at atmospheric pressure. This behavior was able to be reproduced several times and could be a result of the generally weaker cell performance in the test setup at higher current densities. However, a correlation to the higher volumetric gas flows when operating at atmospheric pressure cannot be ruled out. Further investigation with a focus on this aspect is required in order to make a definitive statement.

7. Acknowledgements

The authors would like to thank the Institute of Applied Materials at Helmholtz-Zentrum Berlin GmbH for their help and advice during the experiments and thank HZB for the allocation of neutron radiation beamtime.

8. Literature

[1] Satija, R.; Jacobson, D.; Arif, M. & Werner, S., In situ neutron imaging technique for evaluation of water management systems in operating PEM fuel cells, *Journal of Power Sources ,* **2004***, 129*, 238 - 245

[2] Schröder, A.; Wippermann, K.; Lehnert, W.; Stolten, D.; Sanders, T.; Baumhöfer, T.; Kardjilov, N.; Hilger, A.; Banhart, J. & Manke, I., The influence of gas diffusion layer wettability on direct methanol fuel cell performance: A combined local current distribution and high resolution neutron radiography study, *Journal of Power Sources ,* **2010***, 195*, 4765 - 4771

[3] H. Markötter, I. Manke, R. Kuhn, T. Arlt, N. Kardjilov, M. P. Hentschel, A. Kupsch, A. Lange, C. Hartnig, J. Scholta, J. Banhart: Neutron tomographic investigations of water distributions in polymer electrolyte membrane fuel cell stacks, *Journal of Power Sources,* **2012**, 219, 120-125.

[4] A. Santamaria, H. Y. Tang, J. W. Park, G. G. Park, Y. J. Sohn: 3D neutron tomography of a polymer electrolyte membrane fuel cell under sub-zero conditions, *International Journal of Hydrogen Energy*, **2012**, 37, 10836-10843.

[5] Selamet, O.; Pasaogullari, U.; Spernjak, D.; Hussey, D.; Jacobson, D. & Mat, M. Two-phase flow in a proton exchange membrane electrolyzer visualized in situ by simultaneous neutron radiography and optical imaging, *International Journal of Hydrogen Energy ,* **2013***, 38*, 5823 - 5835

[6] Marcelo Carmo, David L. Fritz, Jürgen Mergel, Detlef Stolten, A comprehensive review on PEM water electrolysis, *International Journal of Hydrogen Energy*, **2013**, 38, 4901-4934

[7] Maximilian Schalenbach, Marcelo Carmo, David L. Fritz, Jürgen Mergel, Detlef Stolten, Pressurized PEM water electrolysis: Efficiency and gas crossover, *International Journal of Hydrogen Energy*, **2013**, 38, 14921-14933

[8] S.A. Grigoriev, V.I. Porembskiy, S.V. Korobtsev, V.N. Fateev, F. Auprêtre, P. Millet, High-pressure PEM water electrolysis and corresponding safety issues, *International Journal of Hydrogen Energy*, **2011**, 36, 2721-2728

[9] Peter D. Lund, Juuso Lindgren, Jani Mikkola, Jyri Salpakari, Review of energy system flexibility measures to enable high levels of variable renewable electricity, *Renewable and Sustainable Energy Reviews*, **2015**, 45, 785-807

[10] P.J.G. Huttenhuis, J.A.M. Kuipers, W.P.M. van Swaaij, The effect of gas-phase density on bubble formation at a single orifice in a two-dimensional gas-fluidized bed, *Chemical Engineering Science*, **1996**, 51, 5273-5288

[11] Tibor Fabian, Jonathan D. Posner, Ryan O'Hayre, Suk-Won Cha, John K. Eaton, Fritz B. Prinz, Juan G. Santiago, The role of ambient conditions on the performance of a planar, air-breathing hydrogen PEM fuel cell, *Journal of Power Sources*, 161, **2006**, 168-182

[12] Luís M.C. Pereira, Antonin Chapoy, Rod Burgass, Mariana B. Oliveira, João A.P. Coutinho, Bahman Tohidi, Study of the impact of high temperatures and pressures on the equilibrium densities and interfacial tension of the carbon dioxide/water system, *The Journal of Chemical Thermodynamics*, Available online 14 May **2015**

[13] Werner Sachs, Volker Meyn, Pressure and temperature dependence of the surface tension in the system natural gas/water principles of investigation and the first precise experimental data for pure methane/water at 25°C up to 46.8 MPa, *Colloids and Surfaces A: Physicochemical and Engineering Aspects*, 94, **1995**, 291-301

[14] Mohammad Sarmadivaleh, Ahmed Z. Al-Yaseri, Stefan Iglauer, Influence of temperature and pressure on quartz–water–CO2 contact angle and CO2–water interfacial tension, *Journal of Colloid and Interface Science*, 441, **2015**, 59-64